SEMARAK ILMU PUBLISHING

Journal of Advanced Research in Applied Mechanics

Journal homepage:
https://semarakilmu.com.my/journals/index.php/appl_mech/index
ISSN: 2289-7895

Prediction of Infiltrating Ductal Carcinoma using Morlet Wavelet Integrated Kolmogorov Arnold Network

Irshad Sikandar Jamadar[1], Krishna Kumar[1], Pratibha Jadhav[2], Pramod Bhalerao[3], Sher Afgan Khan[4,*]

[1] Department of Applied Sciences and Humanities, School of Computing, MIT Arts, Design and Technology University, Pune-412201, India
[2] Department of Applied Sciences and Humanities, School of Engineering and Science, MIT Arts, Design and Technology University, Pune-412201, India
[3] Department of Applied Science and Humanities, Government Polytechnic, Awasari (Kh.), Pune, 412405, India
[4] Department of Mechanical and Aerospace Engineering, Faculty of Engineering, IIUM, Gombak Campus, Kuala Lumpur, Malaysia

ARTICLE INFO

Article history:
Received 4 November 2024
Received in revised form 5 December 2024
Accepted 12 December 2024
Available online 30 December 2024

Keywords:
Breast Cancer Prediction; Kolmogorov-Arnold Network (KAN); Morlet Wavelet Transformations; Histopathological Images; Machine Learning

ABSTRACT

Around the world, breast cancer is among the most terminal type of illness. Infiltrating ductal carcinoma, a case of breast cancer, accounts for 80% of the total diagnosed. The global impact of breast cancer signifies the need for the development of prompt and efficient diagnostic strategies. Morlet wavelet transform is a continuous wavelet transform that captures both spatial and frequency domains. The majority of its applications are in the field of signal processing and image analysis. Image processing helps extract features and examine patterns. This study introduces the model integrating Morlet wavelet transformation within the Kolmogorov Arnold Network (KAN).IDC_regular_ps50_idx5 dataset containing histopathological images is balanced using an augmentation technique. Training of the proposed model is done on the balanced dataset. This integration of Morlet wavelet transform within the Kolmogorov Arnold Network demonstrated impressive performance metrics values. The model achieved a specificity of 91.07%, precision of 90.83%, recall of 88.87%, F1 score of 89.83%, and overall accuracy of 89.97%. The model's output highlights the model's capability in breast cancer prediction.

1. Introduction

Breast cancer is a deadly case of disease affecting women worldwide, as per the study conducted by Kathleen *et al.,* [1]. To increase survival rate, prompt and efficient diagnosis is essential. Tissue structures and cellular irregularities can be observed in histopathological images to differentiate between tissues. Examination of Histopathological photos with the help of Artificial Intelligence can improve diagnostic accuracy. The conventional method of examining histopathological images is time-consuming and susceptible to biases, as concluded by Karim Lekadir *et al.,* [2]. Jadhav and Patil [3] discussed the application of decision trees for developing accurate prediction models. Atam P.

* *Corresponding author.*
E-mail address: sakhan@iium.edu.my

https://doi.org/10.37934/aram.131.1.105118

Dhawan and Dhawan [4] employed wavelet transform instead of traditional Fourier transform. Lokenath Debnath [5] explained how the wavelets can capture information related to frequency and spatial aspects. This ability of wavelets plays a vital role in studying images containing various features and textures. The Morlet wavelet is a continuous wavelet transform employed for examining histopathological images. It combines a wavelet with a Gaussian window to capture subtle and broad features. Its capacity to highlight features at various scales and perspectives is advantageous in histopathological images. The Kolmogorov Arnold Network (KAN) presents a method for constructing networks through the seamless integration of wavelet transforms into its framework. This idea was proposed by Zavareh Bozorgasl and Hao Chen [6]. This integration of wavelet transform enhances the KAN model's ability to analyze images by allowing it to extract subtle and specific details from the given data.

Identification and categorization of breast cancer depend on the correct examination of histopathological images. Regarding the literature, Researchers have conducted predictive modeling using a wide range of machine learning and deep learning strategies on histopathological image datasets. Yungang Zhang *et al.,* [7] studied a mix of neural networks and Random Subspace technique. Fábio Alexandre Spanhol *et al.,* [8] employed Convolutional Neural Networks on BreaKHis dataset. Zhongyi Han *et al.,* [9] constructed a deep-learning model that achieved an impressive accuracy of 93.2% in identifying various breast cancer subtypes. Anuranjeeta *et al.,* [10] emphasized that computer-aided diagnosis CAD systems enhance the precision and effectiveness regarding cancer detection in screening facilities. They achieved this by examining digitized histopathological images to differentiate between non-cancerous and cancerous cells. In their study, Teresa Araújo *et al.,* [11] employed a CNN to analyze biopsy images, reaching an accuracy of 77.8% in overall classification and demonstrating a sensitivity of 95.6% for detecting cancer. In their study, Ferreira *et al.,* [12] applied transfer learning utilizing Inception ResNet V2 to analyze breast cancer histology images. They attained an accuracy rate of 76% when testing on the BACH Challenge blind test set. In their study, Alexander Rakhlin *et al.,* [13] employed deep convolutional neural networks and gradient-boosted trees to analyze breast cancer histopathological images. In a study, Abdullah-Al Nahid *et al.,* [14] proposed a deep neural network model integrated with a restrained Boltzmann machine RBM to have more accurate breast cancer detection through histopathological images. Yaqi Wang *et al.,* [15] applied a hybrid model integrating Convolution Neural Network and Support Vector Machine. Silvia Cascianelli *et al.,* [16] extracted feature vectors with the help of CNN and explored dimensionality reduction techniques like PCA, GRP, and a cross-correlation method to classify histopathological images. Aditya Golatkar *et al.,* [17] applied the pre-trained CNN model Inception_v3 to categorize breast tissue images. Their approach achieved an overall accuracy rate of 85%. Sulaiman Vesal *et al.,* [18] employed the Inception_V3 and ResNet50 neural networks. Dalal Bardou *et al.,* [19] in 2018 studied the effectiveness of traditional learning approaches versus convolution Neural Networks. In 2019, Yuqian Li *et al.,* [20] proposed a method utilizing convolutional neural networks to categorize breast cancer histopathology images. They extracted image segments using clustering techniques. Jonathan de Matos *et al.,* [21] studied a two-step transfer learning approach. They employed the Inception_v3 neural network model, pre-trained on ImageNet for extracting features. Juanying Xie *et al.,* [22] employed deep learning methods such as Inception_V3 and Inception ResNet_V2 and transfer learning. Rui Yan *et al.,* [23] studied a hybrid model combining CNNs and RNNs to differentiate breast cancer images. Their experiment resulted in an accuracy rate of 91.3%. Mesut Toğaçar *et al.,* [24] proposed BreastNet, a convolutional neural network. This model incorporates attention modules and employs data augmentation strategies. Yasin Yari *et al.,* [25] applied transfer learning techniques with ResNet50 and DenseNet121 architectures. Xin Yu Liew *et al.,* [26] presented DLXGB, a model that integrates deep neural network Learning and XGBoost

techniques. Deepika Kumar *et al.,* [27] introduced a voting classifier. The predictions from seven deep neural network learning models, such as CNN variations and transfer learning, were merged. This approach achieved an accuracy of 96.91%. Yan Hu *et al.,* [28] presented an approach to detect breast cancer in histopathological images by employing three-channel features and support vector machines. Elbetel Taye Zewde *et al.,* [29] introduced an automated breast cancer detection system using the ResNet50 model, achieving a classification accuracy of 96.75% for benign and 95% for malignant ones. Swaminathan *et al.,* [30] developed a system that utilized CT scans to forecast the likelihood of lung cancer. The CT images were processed through GAN segmentation. For classification purposes, the VGG16 CNN model was employed. Duodu *et al.,* [31] introduced a system that utilized IoT (Internet of Things) and machine learning. This system combines IoT technology to gather data with a Convolutional Neural Network known as VGG16. Swati B. Bhonde *et al.,* [32] conducted a study on deep learning methods' applicability to forecast cancer outcomes through genome sequencing analysis. Jadhav Pratibha *et al.,* [33] compared the results of two prediction models, regression trees and linear regression, using a dataset from the UCI Machine Learning Repository (UCI). Muthu *et al.,* [34] studied data mining techniques like SVM, KNN, and Decision Tree to detect gastric carcinoma. Khaw *et al.,* [35] analyzed brain MRI images with the help of a modified VGG16 model and Transfer learning. Suhaili *et al.,* [36] applied gray level transformation and brightness manipulation for FPGA-based image processing.

Despite the progress made in leveraging learning for analyzing medical images, especially breast cancer detection, many conventional deep-learning approaches still depend on extracting features from raw pixels or using rudimentary pre-processing methods. These methods overlook essential spatial and frequency domain elements found in histopathological images. Conventional approaches often struggle to capture the details needed to distinguish between non-cancerous and cancerous tissues, leading to limitations in predictive accuracy. Furthermore, while wavelet transforms have shown promise in enhancing feature extraction across different medical imaging fields, their synergy with advanced neural networks such as the Kolmogorov Arnold Network KAN remains an area that has not been extensively explored.

This research aimed to forecast breast cancer by combining Morlet wavelet transformations with a KAN model. The primary focus was evaluating Morlet wavelets' effectiveness in extracting unique characteristics from histopathological images to improve accuracy and dependability. The comprehensive workflow of the study is shown in Figure 1.

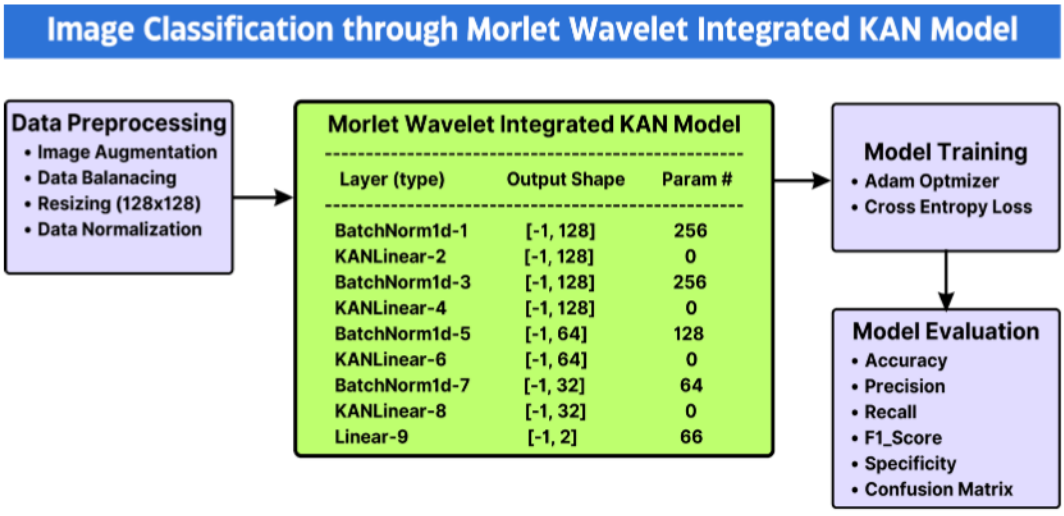

Fig. 1. Comprehensive workflow

2. Dataset and Pre-processing

The IDC_regular_ps50_idx5 dataset is a collection of histopathological image patches sized 50x50 pixels. It is helpful in the detection of Infiltrating Ductal Carcinoma (IDC), which is the most common type of breast cancer. The images in the dataset are labeled as IDC positive for Malignant (Class 1) or IDC negative for Benign (Class 0). The images are organized based on patient IDs, and within each patient's folder, there are subfolders for IDC positive and IDC negative patches. Sample images are shown in Figure 2 and Figure 3

This study uses this dataset consisting of 277,524 histopathological images depicting breast tissue. Out of these images, 198,738 are categorized as benign, while 78,786 are deemed malignant. Due to the significant imbalance between the quantities of benign (Class 0) and malignant (Class 1) images, malignant images are augmented by applying rotation, flipping, scaling, and translation. After using these augmentation methods, the dataset achieved equilibrium with an equal count of benign and malignant images. As a result, the revised dataset now comprises 198,738 benign images and 198,738 malignant images, totaling 297,476 images. The resulting balanced dataset has been organized into a directory called "Balanced," containing subfolders labeled 1 for Malignant (Class 1) samples and 0 for Benign (Class 0) samples.

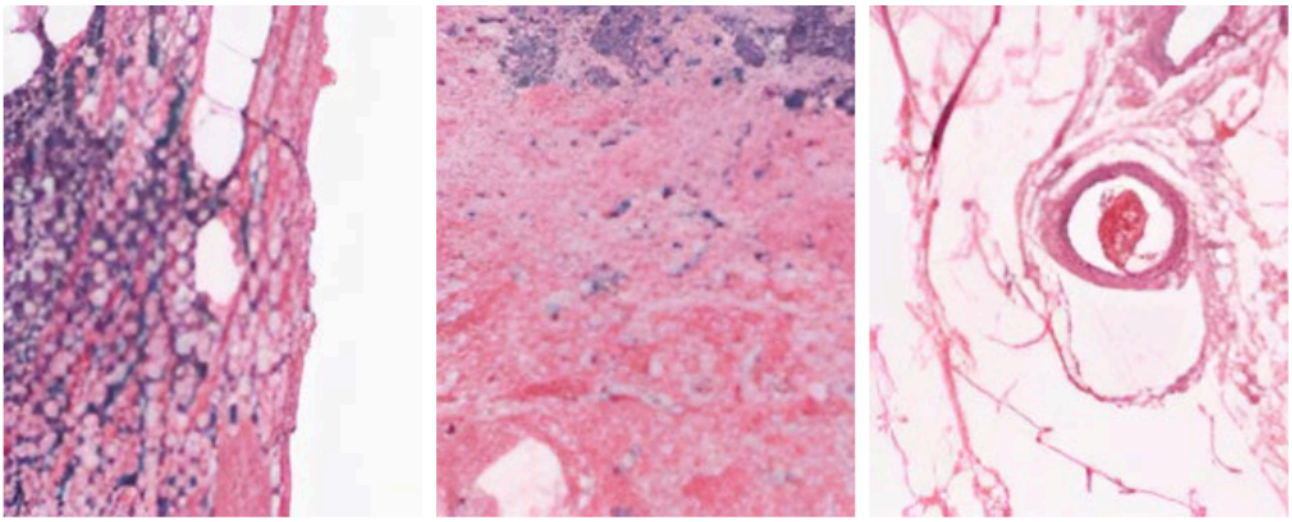

Fig. 2. Sample Benign images

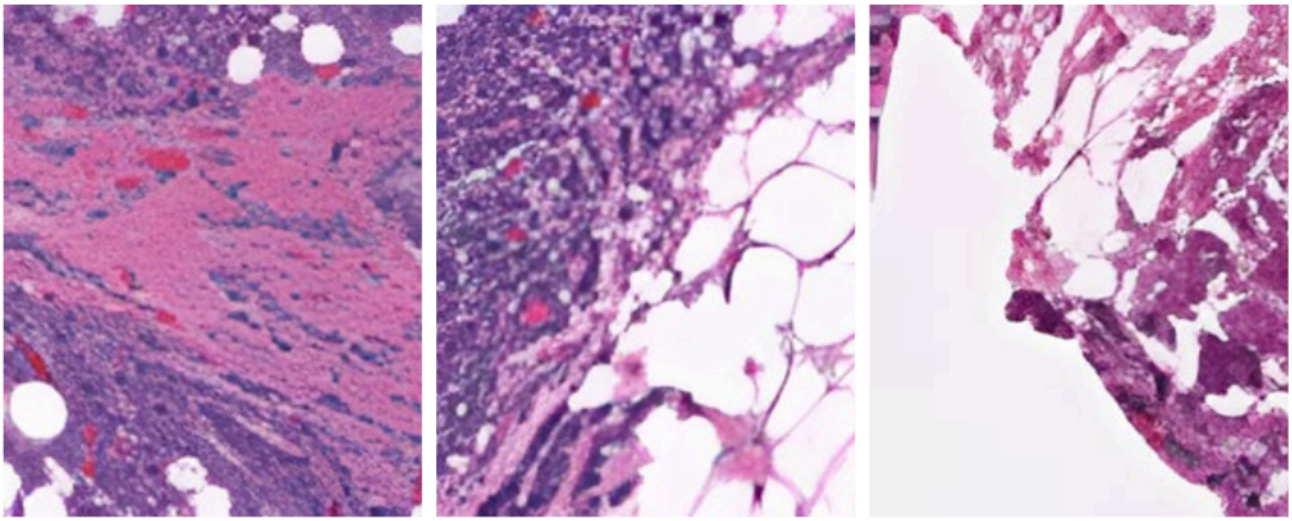

Fig. 3. Sample Malignant images

3. Methodology

3.1 Wavelet Transform

Lokenath Debnath [5] explained that Wavelet transform is a mathematical tool that analyzes the signal into parts at different scale levels. It gives time and frequency information, which is especially valuable for working with non-stationary signals such as images.

3.1.1 Continuous Wavelet Transform (CWT)

The Continuous Wavelet Transform (CWT) of a signal $y(t)$ is defined as,

$$W_y(p,q) = \frac{1}{\sqrt{p}} \int_{-\infty}^{\infty} y(t) \psi^* \left(\frac{t-q}{p} \right) dt \quad (1)$$

Where,

$y(t)$ is the mother wavelet, a function localized in both time and frequency, p is the scale parameter regulating wavelet width q and is the translation parameter handling the position of the wavelet and denoting the complex conjugate ψ .

3.1.2 Discrete Wavelet Transform (DWT)

The Discrete Wavelet Transform (DWT) is a case study of the CWT, using discrete values for the scaling and translating parameters. The DWT of a signal $y(m)$ is given by:

$$W_y[p,q] = \sum_m y(m) \psi_{p,q}[m] \quad (2)$$

Where,

$$\psi_{p,q}[m] = \frac{1}{\sqrt{2j}} \psi \left(\frac{m - q \cdot 2^p}{2p} \right)$$

p and q are integers representing the scaling and translating indices, respectively.

3.1.3 Morlet wavelet

Morlet Wavelet is the type of wavelet transform primarily used in signal processing and image analysis based on the time-frequency analysis of signals. The Morlet wavelet function $\psi(t)$ is defined as:

$$\psi(t) = \pi^{\frac{-1}{4}} e^{i w_0 t} e^{\frac{-t^2}{2}} \quad (3)$$

Where w_o is a dimensionless frequency parameter that determines the central frequency of the wavelet, and i is the imaginary unit?

The Morlet wavelet stands out due to its exceptional frequency representation with a central focus on zero in the frequency domain. This quality makes it highly efficient in detecting oscillatory patterns within signals. One of its capabilities is the simultaneous localization of time and frequency aspects, which proves highly efficient in detecting transient events and specific signal characteristics.

Image processing helps extract features and examine patterns. It preserves the nuances and general texture of an image. It is a valuable tool in diverse areas, such as signal assessment and advanced image processing.

3.1.3 Kolmogorov-Arnold representation theorem

The Kolmogorov-Arnold representation theorem [37] extends the Weierstrass theorem. It suggests that the continuity of multiple functional variables can be expressed through the combination of several functional variables. This idea proposes that a function of variables can be represented using more straightforward functions

$$f(y_1, y_2, y_3, ..., y_n) = \sum_{i=1}^{2m+1} \phi_i \left(\sum_{j=1}^{m} \psi_{ij}(y_j) \right) \tag{4}$$

Where f the function is to be approximated ψ_{ij} are continuous functions.

3.2 Wavelet-KAN Model Architecture by *Zavareh Bozorgasl and Hao Chen [6]*

Wavelet transformations can be smoothly incorporated into the structure of the Kolmogorov-Arnold Network. This integration allows for the effective extraction of specific features from histopathological images. In this architecture, every layer incorporates a KAN Linear module that substitutes conventional fully connected linear layers. Instead of applying transformations, the KAN Linear module utilizes wavelet transforms on the inputs as they progress through the network. This assures the model retains key details about frequency and time-frequency aspects before applying the activation functions. The Morlet wavelet, known for its localization capabilities, is specifically designed for these layers, enabling the extraction of transient and complex characteristics across different scales.

We utilize a Kolmogorov Arnold Network (KAN) structure (Table 1) that incorporates Morlet wavelets instead of conventional weights in the linear layers. What sets this method apart is its use of the mathematical characteristics of Morlet wavelets for extracting features directly within the neural network. Instead of feeding in wavelet data, we process the raw input through layers that employ Morlet wavelets to extract features dynamically. Within the Kolmogorov Arnold Network KAN framework that incorporates wavelet transformations, the process starts at the layer that handles pre-processed images referred to as X. Every image is thoroughly examined in the Wavelet Transformation Layer by applying the wavelet transform function. This function can be represented as ψ .

$$W_x(a,b) = \frac{1}{\sqrt{a}} \int_{-\infty}^{\infty} X(t) \psi^* \left(\frac{t-b}{a} \right) dt \tag{5}$$

The process involves breaking down images into wavelet coefficients representing various frequency elements, enabling a thorough examination of the picture's intricate and subtle details. After the wavelet transformation, the modified coefficients go through several hidden layers for further processing. Each hidden layer l applies a series of changes to the wavelet coefficients. Each hidden layer's output h_l can be represented as,

$$h_l = \psi(\omega_l \cdot O_{l-1} + b_l) \tag{6}$$

where,

ω_l is the l-th layer weight matrix.

O_{l-1} is the previous layer output.

b_l is the l-th layer bias vector.

ψ represents the wavelet transform applied to the linear integration of inputs. Here, ψ is used on the weighted sum of inputs, permitting the network to capture intricate characteristics and trends in the images transformed through wavelet analysis.

In terms of architecture, the neural network incorporates a BatchNorm1d layer (BatchNorm1d-1) that standardizes the inputs. This normalization process aids in maintaining equilibrium in the dataset throughout training and promotes quicker convergence. This layer comprises 256 parameters obtained by computing the mean and variance for normalizing 128 features. In the subsequent layer, named KANLinear-2, the Morlet wavelet transformation is utilized in place of conventional neurons. This choice leads to a parameter count of 0, as wavelets are established mathematical functions. Following this step, BatchNorm1d-3 applies normalization to the output of KANLinear-2 just like BatchNorm1d-1 without using conventional neurons. In KANLinear-4, we again apply the Morlet wavelet transformation without any trainable parameters or neurons being involved. The sequence repeats with BatchNorm1d layers, taking turns with KANLinear layers. Each BatchNorm1d layer normalizes the input data while each KANLinear layer performs predetermined Morlet wavelet transformations. Throughout the process, the dimensionality of the feature space is decreased (from 128 to 64 and subsequently to 32) through the application of BatchNorm1d layers. These layers condense the extracted features while retaining crucial information. This gradual reduction enables the network to hone in on the features streamlining its decision-making workflow.

The final layer is a classification layer known as Linear-9. It has 66 parameters and utilizes weights that can be adjusted to determine whether the input is benign or malignant. This layer employs a sigmoid activation function.

$$\hat{y} = \sigma(\omega_{out} \cdot O_L + b_{out}) \tag{7}$$

Where,

ω_{out} and b_{out} are the weights and biases of the output layer and the sigmoid function. The sigmoid function takes the last mix of features and converts them into a probability score ranging from 0 to 1. This score indicates the probability of an image being categorized into a particular category. Through the utilization of this approach, the procedure ensures that the model effectively utilizes the wavelet-transformed attributes along with the modifications in the hidden layer to achieve accurate and reliable classifications.

Implementing Morlet wavelets in KAN offers several advantages. One notable advantage is the minimization of the number of parameters, with the whole network consisting of just 770 parameters, mainly concentrated in the normalization layers. Replacing traditional weight matrices with Morlet wavelets decreases the number of parameters required to be adjusted, making the training process more efficient. In this approach, wavelets enhance the capacity to generalize by reducing the chances of overfitting. This aspect is vital in medical imaging scenarios where data is often limited.

3.1.4 Model evaluation

The KAN wavelet model was trained using a dataset of histopathological images over 50 epochs. The data was passed into the model in batches to improve efficiency and optimize memory usage. Images were simultaneously processed to complete the training process rapidly. The main objective of the model was to reduce loss, which was calculated through the loss function (cross-entropy).

Various metrics commonly used in binary classification were employed to evaluate the effectiveness of the Morlet KAN model. Precision calculates the ratio of accurately predicted cancerous tissues to all predicted cases. A high precision score reflects the model's ability to reduce false positives. Sensitivity, known as recall, assesses how well the model can accurately detect malignant tissues. It is the ratio of true positive cases out of all the real positive instances. Recall highlights how the model identifies cancerous tissues without missing any cases. The F1 score uses both recall and precision to offer a perspective on the effectiveness of the models. Precision and recall can occasionally be at odds with each other. However, the F1 score provides a balanced assessment by assigning importance to both measures.

Moreover, the metric accuracy evaluates the model's performance. Accuracy assesses how well the model classifies both classes (1 and 0) regarding all instances in the dataset. The combined analysis of these metrics evaluates the Morlet KAN model.

4. Results and Discussion

4.1 Training and Validation Loss

This section discusses training, validating, and testing results of the Morlet KAN model.

The loss plot in Figure 4 shows a continuous decrease in training and validation losses, establishing that the model has effectively learned to minimize classification mistakes throughout the training process. The loss value is typically high at the beginning of training, although this is expected. It soon decreases rapidly, showing that the model is improving its optimization attempts. The starting loss is around 0.6963 for the training set and approximately 0.6918 for the validation set. By the final epoch, the training loss decreased to about 0.1410, while the validation loss settled at 0.3321. This low validation loss suggests that the model has effectively learned the data without overfitting significantly, as indicated by the minimal divergence between the training and validation loss curves. The smooth convergence of both curves showcases the stability and effectiveness of Morlet wavelet feature extraction in supporting model learning. Typically, overfitting is marked by a gap between these two curves, but such an occurrence is not observed in this case.

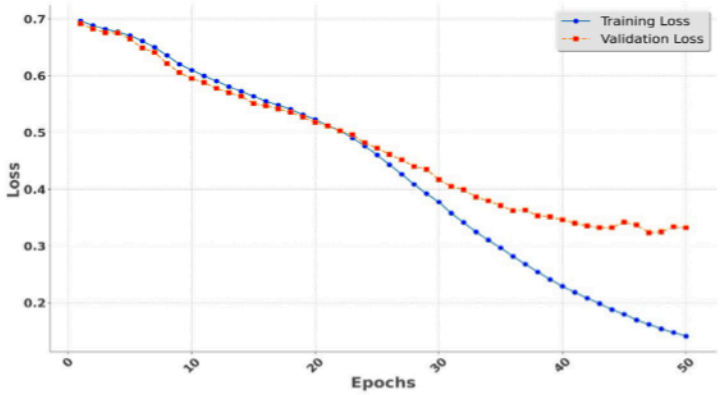

Fig. 4. Training Vs. validation loss over epochs

4.2 Training and Validation Accuracy

The accuracy graph (Figure 5) shows that the model steadily improves over the epochs for both the training and validation sets. Initially, it starts with an accuracy of approximately 0.5194, indicating random guessing, but quickly increases as it learns relevant features. In the early stages, the accuracy is around 0.5194, reflecting a point where the model faces challenges in classifying tasks. By the end, training accuracy is 0.9470, and validation accuracy is 0.8989. The slight difference between training and validation accuracy suggests that the model is well-balanced and does not overfit the training data. The final validation accuracy of 0.8989 indicates that the model effectively operates on unseen data. This high accuracy level and minimal variations throughout the epochs indicate that the Morlet wavelet transformation effectively enhances features, enabling the model to distinguish between classes.

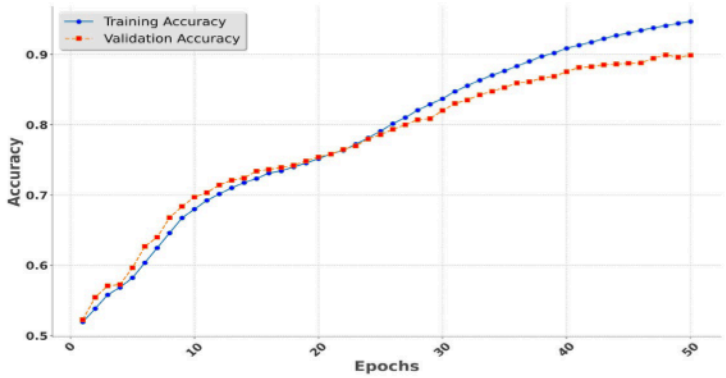

Fig. 5. Training Vs. validation accuracy over epochs

4.3 Training and Validation Precision

Precision evaluates the proportion of predicted samples that are genuinely positive. The precision chart (Figure 6) shows consistent values during the training and Validation phases. By the final epoch, the training precision is 0.9543, and the validation precision is 0.9035. A precision value indicates that the model is effectively reducing false positives. This is most important in healthcare settings where incorrectly classifying a benign case as malignant could lead to unnecessary concern or action. The high precision value indicates that the model accurately detects malignant cases while minimizing misclassifications of benign ones. The steady rise and absence of variations in precision over epochs indicate a reliable model.

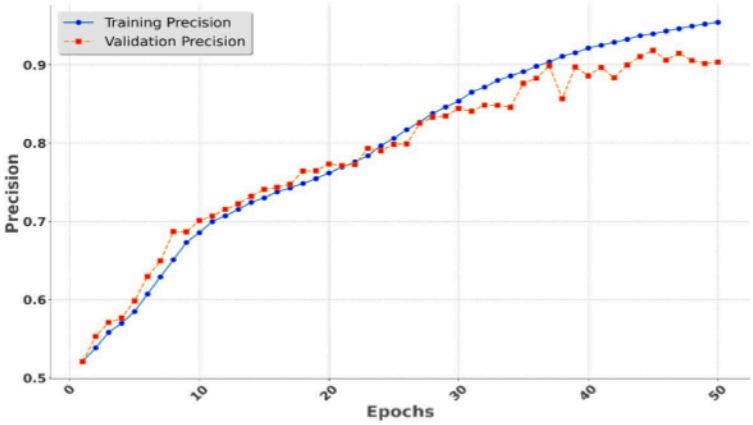

Fig. 6. Training Vs. validation precision over epochs

4.4 Training and Validation Recall

In this context, recall plays a role in assessing how well the model can accurately identify all true positive instances, specifically in capturing all malignant cases. The recall chart (Figure 7) demonstrates that the model achieves recall scores, suggesting that it correctly classifies most positive samples. It reaches approximately 0.9390 for training after the training phase. This indicates that the model effectively recognizes nearly all malignant cases with very few false negatives (malignant cases misclassified as benign). A high recall rate in cancer diagnosis is crucial to ensure that no malignant cases go undetected since such an oversight could have serious consequences. The relatively stable recall rates suggest that the Morlet wavelet transformation has proven advantageous in extracting essential features associated with the positive class (malignant cases).

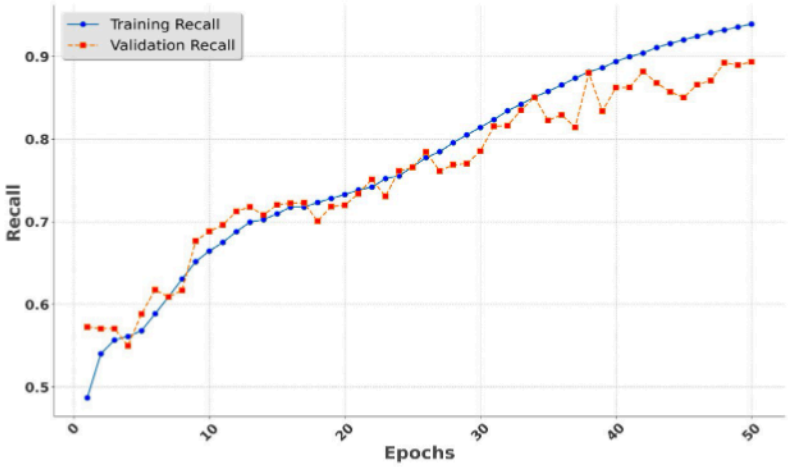

Fig. 7. Training Vs. validation recall over epochs

4.5 Training and Validation F1_Score

Recall and precision averaged together give F1_Score. It offers a perspective on how good a model is. From (Figure 8), the Final F1 Score is around 0.9466 after training. This impressive F1 score showcases the model's ability to strike precision and recall balance, which is crucial to avoid the dilemma of high precision compromising recall or vice versa. With the final F1 score being closely aligned with both precision and recall (0.9543 and 0.939, respectively), the model consistently finds true positives while minimizing false positives.

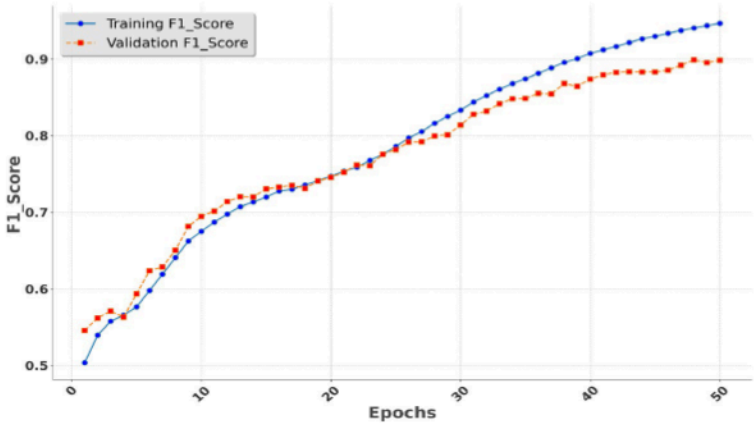

Fig. 8. Training Vs. validation F1_score over epochs

$$Accuracy = \frac{TP + TN}{TP + TN + FP + FN} = \frac{35247 + 36280}{35247 + 36280 + 3557 + 4411} = 0.8997 \quad (8)$$

$$\Pr ecision = \frac{TP}{TP + FP} = \frac{35247}{35247 + 3557} = 0.9083 \quad (9)$$

$$\mathrm{Re}\, call = \frac{TP}{TP + FN} = \frac{35247}{35247 + 4411} = 0.8887 \quad (10)$$

$$Specificity = \frac{TN}{TN + FP} = \frac{36280}{36280 + 3557} = 0.9107 \quad (11)$$

$$F_{1\_}Score = 2 \times \frac{(\mathrm{Re}\, call \times \Pr ecision)}{(\Pr ecision + \mathrm{Re}\, call)} = 2 \times \frac{0.9083 \times 0.8887}{0.9083 + 0.8887} = 0.8983 \quad (12)$$

4.6 Confusion Matrix

The confusion matrix (Figure 9) offers insight into how the classification is performed by displaying the true positives, true negatives, false positives, and false negatives for both the benign and malignant classes. True Positives (Malignant Correctly Classified): the matrix reveals that a significant portion of malignant cases are accurately identified at an accuracy rate of 88.87% for this category. True Negatives (Benign Correctly Classified) Approximately 91.07% of benign cases are also correctly recognized, demonstrating the model's effectiveness across both categories. False Positives (Benign Misclassified as Malignant): the incidence of false positives is relatively low (around 8.92%), indicating the model's precision. False Negatives (Malignant Misclassified as Benign) Likewise, false negatives are minimal (around 11.12%), which aligns with the high recall metric. The confusion matrix reveals that the model's performance is strong in both categories, with only a few misclassifications. While these errors are relatively minor, they could still deserve consideration. Using the Morlet wavelet technique seems to assist the model in identifying key features specific to each class that reduce mistakes overall.

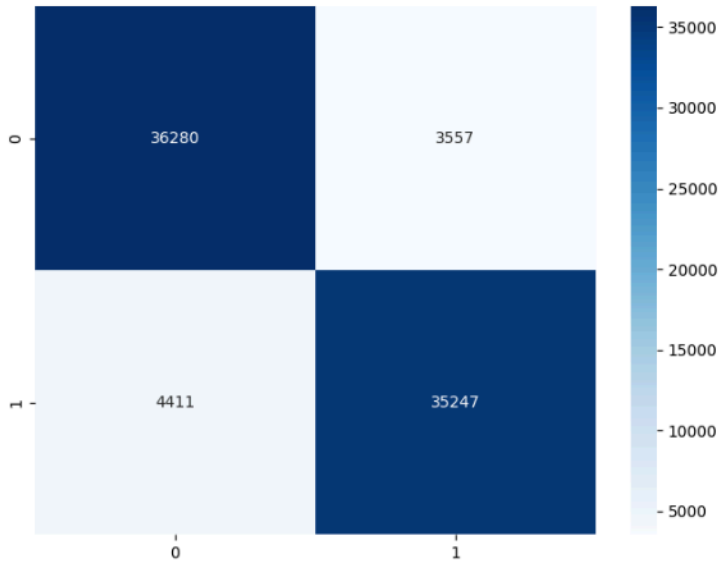

Fig. 9. Confusion matrix

5. Conclusion

This research concludes that integrating Morlet wavelet transformation in the Kolmogorov Arnold Network achieved impressive performance metrics. Morlet wavelet increased the model's ability to extract characteristics from histopathological images, essential for breast cancer diagnosis. The effectiveness of the Morlet wavelet in feature extraction has played a role in the success of the classification model. The model achieved precision, recall, F1 score, specificity, and accuracy at 90.83%, 88.87%, 89.83%, 91.08%, and 89.97%, respectively. The low loss and consistent validation metrics indicate strong generalization without overfitting. In addition, the confusion matrix shows that the model has a low misclassification rate. Wavelet transformations enhance accuracy in diagnosing cancerous areas. This allows for detecting tumors, potentially leading to prompt treatment actions and better patient results. Integrating wavelet transformations into the KAN framework may present difficulties regarding computational requirements, particularly in real-time settings and limited resources. However, despite these challenges, the KAN model integrated by Morlet wavelet transformations shows potential as a promising tool that deserves further testing in future research and comparative studies to evaluate its effectiveness in real-world clinical settings.

6. Future Work

Further investigation based on these results is required. The use of different wavelets could improve feature extraction and diagnostic accuracy. Integrating data sources like structural and functional imaging through wavelet processing might enhance cancer diagnosis and staging precision. Optimizing the model for real-time image analysis could facilitate its implementation in clinical environments, supporting timely and informed decisions. These advancements promise to enhance the efficacy of diagnostic tools significantly, leading to better patient management and outcomes.

Acknowledgment

We sincerely thank Prof. Javed Shoukat Shaikh and Prof. Khaizer Ahmed Pathan for their invaluable guidance and insightful suggestions during this study.

References

[1] Cronin, Kathleen A., Susan Scott, Albert U. Firth, Hyuna Sung, S. Jane Henley, Recinda L. Sherman, Rebecca L. Siegel et al. "Annual report to the nation on the status of cancer, part 1: National cancer statistics." *Cancer* 128, no. 24 (2022): 4251-4284. https://doi.org/10.1002/cncr.34479

[2] Lekadir, Karim, Richard Osuala, Catherine Gallin, Noussair Lazrak, Kaisar Kushibar, Gianna Tsakou, Susanna Aussó et al. "FUTURE-AI: guiding principles and consensus recommendations for trustworthy artificial intelligence in medical imaging." *arXiv preprint arXiv:2109.09658* (2021). https://doi.org/10.48550/arXiv.2109.09658

[3] Jadhav, Pratibha Vijay, and Vaishali Vilas Patil. *Application of Decision Tree for Developing Accurate Prediction Models*. Ashok Yakkaldevi, 2022.

[4] Dhawan, Atam P. "Wavelet Transform and Its Applications in Medical Image Analysis." In *Principles And Advanced Methods In Medical Imaging And Image Analysis*, pp. 437-454. 2008. https://doi.org/10.1142/9789812814807_0018

[5] Debnath, Lokenath, and Firdous Ahmad Shah. *Wavelet transforms and their applications*. Vol. 434. New York: Birkhäuser, 2015.

[6] Bozorgasl, Zavareh, and Hao Chen. "Wav-kan: Wavelet kolmogorov-arnold networks." *arXiv preprint arXiv:2405.12832* (2024). https://doi.org/10.48550/arXiv.2405.12832

[7] Zhang, Yungang, Bailing Zhang, and Wenjin Lu. "Breast cancer classification from histological images with multiple features and random subspace classifier ensemble." In *AIP Conference Proceedings*, vol. 1371, no. 1, pp. 19-28. American Institute of Physics, 2011. https://doi.org/10.1063/1.3596623

[8] Spanhol, Fabio Alexandre, Luiz S. Oliveira, Caroline Petitjean, and Laurent Heutte. "Breast cancer histopathological image classification using convolutional neural networks." In *2016 international joint conference on neural networks (IJCNN)*, pp. 2560-2567. IEEE, 2016.

[9] Han, Zhongyi, Benzheng Wei, Yuanjie Zheng, Yilong Yin, Kejian Li, and Shuo Li. "Breast cancer multi-classification from histopathological images with structured deep learning model." *Scientific reports* 7, no. 1 (2017): 4172. https://doi.org/10.1038/s41598-017-04075-z

[10] Shukla, K. K., Anoop Tiwari, and Shiru Sharma. "Classification of histopathological images of breast cancerous and non cancerous cells based on morphological features." *Biomedical and Pharmacology Journal* 10, no. 1 (2017): 353-366. https://dx.doi.org/10.13005/bpj/1116

[11] Araújo, Teresa, Guilherme Aresta, Eduardo Castro, José Rouco, Paulo Aguiar, Catarina Eloy, António Polónia, and Aurélio Campilho. "Classification of breast cancer histology images using convolutional neural networks." *PloS one* 12, no. 6 (2017): e0177544. https://doi.org/10.1371/journal.pone.0177544

[12] Ferreira, Carlos A., Tânia Melo, Patrick Sousa, Maria Inês Meyer, Elham Shakibapour, Pedro Costa, and Aurélio Campilho. "Classification of breast cancer histology images through transfer learning using a pre-trained inception resnet v2." In *International conference image analysis and recognition*, pp. 763-770. Cham: Springer International Publishing, 2018. https://doi.org/10.1007/978-3-319-93000-8_86

[13] Rakhlin, Alexander, Alexey Shvets, Vladimir Iglovikov, and Alexandr A. Kalinin. "Deep convolutional neural networks for breast cancer histology image analysis." In *Image Analysis and Recognition: 15th International Conference, ICIAR 2018, Póvoa de Varzim, Portugal, June 27–29, 2018, Proceedings 15*, pp. 737-744. Springer International Publishing, 2018. https://doi.org/10.1007/978-3-319-93000-8_83

[14] Nahid, Abdullah-Al, Aaron Mikaelian, and Yinan Kong. "Histopathological breast-image classification with restricted Boltzmann machine along with backpropagation." *Biomedical Research* 29, no. 10 (2018): 2068-2077. http://dx.doi.org/10.4066/biomedicalresearch.29-17-3903

[15] Wang, Yaqi, Lingling Sun, Kaiqiang Ma, and Jiannan Fang. "Breast cancer microscope image classification based on CNN with image deformation." In *Image Analysis and Recognition: 15th International Conference, ICIAR 2018, Póvoa de Varzim, Portugal, June 27–29, 2018, Proceedings 15*, pp. 845-852. Springer International Publishing, 2018. https://doi.org/10.1007/978-3-319-93000-8_96

[16] Cascianelli, Silvia, Raquel Bello-Cerezo, Francesco Bianconi, Mario L. Fravolini, Mehdi Belal, Barbara Palumbo, and Jakob N. Kather. "Dimensionality reduction strategies for cnn-based classification of histopathological images." In *Intelligent Interactive Multimedia Systems and Services 2017 10*, pp. 21-30. Springer International Publishing, 2018. https://doi.org/10.1007/978-3-319-59480-4_3

[17] Golatkar, Aditya, Deepak Anand, and Amit Sethi. "Classification of breast cancer histology using deep learning." In *Image Analysis and Recognition: 15th International Conference, ICIAR 2018, Póvoa de Varzim, Portugal, June 27–29, 2018, Proceedings 15*, pp. 837-844. Springer International Publishing, 2018. https://doi.org/10.1007/978-3-319-93000-8_95

[18] Vesal, Sulaiman, Nishant Ravikumar, AmirAbbas Davari, Stephan Ellmann, and Andreas Maier. "Classification of breast cancer histology images using transfer learning." In *Image Analysis and Recognition: 15th International Conference, ICIAR 2018, Póvoa de Varzim, Portugal, June 27–29, 2018, Proceedings 15*, pp. 812-819. Springer International Publishing, 2018. https://doi.org/10.1007/978-3-319-93000-8_92

[19] Bardou, Dalal, Kun Zhang, and Sayed Mohammad Ahmad. "Classification of breast cancer based on histology images using convolutional neural networks." *Ieee Access* 6 (2018): 24680-24693.

[20] Li, Yuqian, Junmin Wu, and Qisong Wu. "Classification of breast cancer histology images using multi-size and discriminative patches based on deep learning." *Ieee Access* 7 (2019): 21400-21408.

[21] De Matos, Jonathan, Alceu de S. Britto, Luiz ES Oliveira, and Alessandro L. Koerich. "Double transfer learning for breast cancer histopathologic image classification." In *2019 international joint conference on neural networks (IJCNN)*, pp. 1-8. IEEE, 2019.

[22] Xie, Juanying, Ran Liu, Joseph Luttrell IV, and Chaoyang Zhang. "Deep learning based analysis of histopathological images of breast cancer." *Frontiers in genetics* 10 (2019): 80.

[23] Yan, Rui, Fei Ren, Zihao Wang, Lihua Wang, Tong Zhang, Yudong Liu, Xiaosong Rao, Chunhou Zheng, and Fa Zhang. "Breast cancer histopathological image classification using a hybrid deep neural network." *Methods* 173 (2020): 52-60. https://doi.org/10.1016/j.ymeth.2019.06.014

[24] Toğaçar, Mesut, Kutsal Baran Özkurt, Burhan Ergen, and Zafer Cömert. "BreastNet: A novel convolutional neural network model through histopathological images for the diagnosis of breast cancer." *Physica A: Statistical Mechanics and its Applications* 545 (2020): 123592. https://doi.org/10.1016/j.physa.2019.123592

[25] Yari, Yasin, Thuy V. Nguyen, and Hieu T. Nguyen. "Deep learning applied for histological diagnosis of breast cancer." *IEEE Access* 8 (2020): 162432-162448.

[26] Liew, Xin Yu, Nazia Hameed, and Jeremie Clos. "An investigation of XGBoost-based algorithm for breast cancer classification." *Machine Learning with Applications* 6 (2021): 100154. https://doi.org/10.1016/j.mlwa.2021.100154
[27] Kumar, Deepika, and Usha Batra. "Breast cancer histopathology image classification using soft voting classifier." In *Proceedings of 3rd International Conference on Computing Informatics and Networks: ICCIN 2020*, pp. 619-631. Singapore: Springer Singapore, 2021. https://doi.org/10.1007/978-981-15-9712-1_53
[28] Hao, Yan, Shichang Qiao, Li Zhang, Ting Xu, Yanping Bai, Hongping Hu, Wendong Zhang, and Guojun Zhang. "Breast cancer histopathological images recognition based on low dimensional three-channel features." *Frontiers in oncology* 11 (2021): 657560.
[29] Zewde, Elbetel Taye, and Gizeaddis Lamesgin Simegn. "Automatic diagnosis of breast cancer from histopathological images using deep learning technique." In *Advances of Science and Technology: 9th EAI International Conference, ICAST 2021, Hybrid Event, Bahir Dar, Ethiopia, August 27–29, 2021, Proceedings, Part I*, pp. 619-634. Springer International Publishing, 2022. https://doi.org/10.1007/978-3-030-93709-6_42
[30] Swaminathan, Vishnu Priyan, Ramesh Balasubramani, S. Parvathavarthini, Vidhya Gopal, Kanagaselvam Raju, Tamil Selvan Sivalingam, and Sounder Rajan Thennarasu. "GAN Based Image Segmentation and Classification Using Vgg16 for Prediction of Lung Cancer." *Journal of Advanced Research in Applied Sciences and Engineering Technology* 35, no. 1 (2024): 45-61. https://doi.org/10.37934/araset.35.1.4561
[31] Duodu, Nana Yaw, Warish D. Patel, and Amit Ganatra. "Advancements in Telehealth: Enhancing breast cancer detection and health automation through smart integration of iot and cnn deep learning in residential and healthcare settings." *Journal of Advanced Research in Applied Sciences and Engineering Technology* 45, no. 2 (2025): 214-226. https://doi.org/10.37934/araset.45.2.214226
[32] Bhonde, Swati B., and Jayashree R. Prasad. "Deep Learning Techniques in Cancer Prediction Using Genomic Profiles." In *2021 6th International Conference for Convergence in Technology (I2CT)*, pp. 1-9. IEEE, 2021.
[33] Jadhav, Pratibha, Dr Vaishali Patil, and Dr Sharad Gore. "A comparative study of linear regression and regression tree." In *2nd International Conference on Communication & Information Processing (ICCIP)*. 2020. http://dx.doi.org/10.2139/ssrn.3645883
[34] Muthu, Shanmuga Pillai Murutha, and Sellappan Palaniappan. "Categorization of Early Detection Classifiers for Gastric Carcinoma through Data Mining Approaches." *Journal of Advanced Research in Computing and Applications* 32, no. 1 (2023): 1-12. https://doi.org/10.37934/arca.32.1.112
[35] Khaw, Li Wen, and Shahrum Shah Abdullah. "Mri Brain Image Classification Using Convolutional Neural Networks and Transfer Learning." *Journal of Advanced Research in Computing and Applications* 31, no. 1 (2023): 20-26. https://doi.org/10.37934/arca.31.1.2026
[36] Suhaili, Shamsiah, Joyce Shing Yii Huong, Asrani Lit, Kuryati Kipli, Maimun Huja Husin, Mohamad Faizrizwan Mohd Sabri, and Norhuzaimin Julai. "Development of digital image processing algorithms via fpga implementation." *Semarak International Journal of Electronic System Engineering* 3, no. 1 (2024): 28-45. https://doi.org/10.37934/sijese.3.1.2845
[37] Tikhomirov, V. M. "On the representation of continuous functions of several variables as superpositions of continuous functions of one variable and addition." In *Selected Works of AN Kolmogorov*, pp. 383-387. Springer, Dordrecht, 1991.